10-30-2008

Plurality of principal angles for a given pseudo-Brewster angle when polarized light is reflected at a dielectric-conductor interface

R. M.A. Azzam
University of New Orleans, razzam@uno.edu

A. Alsamman
University of New Orleans, aalsamma@uno.edu

Recommended Citation
R. M. A. Azzam and A. Alsamman, "Plurality of principal angles for a given pseudo-Brewster angle when polarized light is reflected at a dielectric-conductor interface," J. Opt. Soc. Am. A 25, 2858-2864 (2008)

Plurality of principal angles for a given pseudo-Brewster angle when polarized light is reflected at a dielectric–conductor interface

R. M. A. Azzam* and A. Alsamman

Department of Electrical Engineering, University of New Orleans, New Orleans, Louisiana 70148, USA
**Corresponding author: razzam@uno.edu*

Received July 17, 2008; accepted September 12, 2008;
posted September 22, 2008 (Doc. ID 98934); published October 30, 2008

The pseudo-Brewster angle ϕ_{pB} of minimum reflectance for p-polarized light and the principal angle $\bar{\phi}$ at which incident linearly polarized light of the proper azimuth is reflected circularly polarized are considered as functions of the complex relative dielectric function ε of a dielectric–conductor interface over the entire complex ε plane. In particular, the spread of $\bar{\phi}$ for a given ϕ_{pB} is determined, and the maximum difference $(\bar{\phi}-\phi_{pB})_{\max}$ is obtained as a function of ϕ_{pB}. The maximum difference $(\bar{\phi}-\phi_{pB})_{\max}$ approaches 45° and 0 in the limit as $\phi_{pB}\to 0$ and 90°, respectively. For $\phi_{pB}<22.666°$, multiple principal angles $\bar{\phi}_i$, $i=1,2,3$, appear for each ε in a subdomain of fractional optical constants. This leads to an elaborate pattern of multiple solution branches for the difference $\bar{\phi}_i-\phi_{pB}$, $i=1,2,3$, as is illustrated by several examples. © 2008 Optical Society of America

OCIS codes: 120.5700, 240.0240, 240.2130, 260.0260, 260.3910, 260.5430.

1. INTRODUCTION

The reflection of monochromatic p- and s-polarized light at an angle ϕ by the planar interface between a transparent medium of incidence (ambient) of refractive index n_0 and an absorbing medium of refraction (substrate) of complex refractive index $N_1=n_1-jk_1$ is governed by the well-known complex-amplitude Fresnel reflection coefficients [1–3]:

$$r_p=\frac{\varepsilon\cos\phi-(\varepsilon-\sin^2\phi)^{1/2}}{\varepsilon\cos\phi+(\varepsilon-\sin^2\phi)^{1/2}}, \tag{1}$$

$$r_s=\frac{\cos\phi-(\varepsilon-\sin^2\phi)^{1/2}}{\cos\phi+(\varepsilon-\sin^2\phi)^{1/2}}, \tag{2}$$

$$\varepsilon={N_1}^2/{n_0}^2=(n-jk)^2=\varepsilon_r-j\varepsilon_i. \tag{3}$$

For a given value of the complex relative dielectric function ε, which is characteristic of a given interface at a given wavelength, the amplitude reflectance $|r_p|$ of p-polarized light as a function of ϕ reaches a minimum at the *pseudo-Brewster angle* (PBA) ϕ_{pB}. If the medium of refraction is also transparent, $\varepsilon_i=0$, the minimum reflectance is zero, $|r_p|_{\min}=0$, and the PBA ϕ_{pB} reverts back to the usual Brewster angle $\phi_B=\tan^{-1}\sqrt{\varepsilon_r}$. Recall that for any ε the amplitude reflectance $|r_s|$ of s-polarized light increases monotonically as a function of ϕ between normal and grazing incidence, $0\leqslant\phi\leqslant 90°$.

The first correct derivation of the relation between ϕ_{pB} and complex ε (which replaces Brewster's law) is believed to be that of Humphreys–Owen [4], as was noted by Holl [5]. Continued interest in this salient feature of the reflection of p-polarized light (and other electromagnetic waves) at a dielectric–conductor interface has led to several subsequent derivations [6–9].

Another important and distinct angle of incidence is the *principal angle* (PA) $\bar{\phi}$ at which incident linearly polarized light of the proper azimuth (called the *principal azimuth* $\bar{\psi}$) is reflected circularly polarized [1–3,10]. This occurs when the differential reflection phase shift Δ of p- and s-polarized light is quarter-wave, i.e.,

$$\Delta=\delta_p-\delta_s=90°,$$

$$\delta_p=\arg(r_p),\qquad \delta_s=\arg(r_s). \tag{4}$$

The ratio of complex p and s reflection coefficients, also known as the ellipsometric function ρ [2], is obtained from Eqs. (1) and (2) as

$$\rho=r_p/r_s=\frac{\sin\phi\tan\phi-(\varepsilon-\sin^2\phi)^{1/2}}{\sin\phi\tan\phi+(\varepsilon-\sin^2\phi)^{1/2}}. \tag{5}$$

At the principal angle, $\phi=\bar{\phi}$, ρ becomes pure imaginary,

$$\rho=\bar{\rho}=j\tan\bar{\psi}. \tag{6}$$

For a given complex ε, the PA, $\bar{\phi}$, is determined by solving a cubic equation [10]:

$$a_3u^3+a_2u^2+a_1u+a_0=0, \tag{7}$$

$$a_0={\varepsilon_r}^2+{\varepsilon_i}^2,\qquad a_1=-2(a_0+\varepsilon_r),$$

$$a_2=a_0+4\varepsilon_r+1,\qquad a_3=-2(\varepsilon_r+1), \tag{8}$$

$$u = \sin^2\bar{\phi}. \tag{9}$$

Over much of the complex plane, Eqs. (7)–(9) yield only one acceptable root ($0<u<1$), hence one PA $\bar{\phi}$, for each ε. However, as has been noted in [5,10], there exists a small but important region of fractional optical constants ($0<|\varepsilon_r|$, $|\varepsilon_i|<1$) within which three distinct PAs exist for each complex ε. This domain of multiple principal angles (MPAs), shown highlighted in Fig. 1, is bounded by the real axis, $\varepsilon_i=0$, and the curve whose parametric equation is given by [10]

$$\varepsilon_r = u + \frac{u^3(u-2)}{(1-u)^3},$$

$$\varepsilon_i = \frac{(2u^6-4u^5+u^4)^{1/2}}{(1-u)^3},$$

$$0 \leqslant u \leqslant 1 - \frac{1}{\sqrt{2}} = 0.293. \tag{10}$$

Equations (10) represent the locus of all possible values of complex ε for which two of the three principal angles, $\bar{\phi}=\sin^{-1}\sqrt{u}$, coincide; this locus is represented by the dashed curve in Fig. 1. The cusp point P corresponds to $u=1/4$ and is located at $\varepsilon=(5/27,\sqrt{2}/27)$. Fractional optical constants are encountered for many materials in the vacuum UV and x-ray spectral regions [11,12] and also in attenuated or total internal reflection when light is incident from an optically dense medium [13].

Because of approximate formulations used in metal optics, the PBA and PA are sometimes erroneously presumed to be the same. In this paper the difference between these two angles, $\bar{\phi}-\phi_{pB}$, is thoroughly investigated as a function of complex ε. This is accomplished in Section 2 by deliberately holding ϕ_{pB} constant and determining all possible values of the associated PA $\bar{\phi}$. The maximum difference $(\bar{\phi}-\phi_{pB})_{\max}$ is also determined as a function of ϕ_{pB}. Unusual results are obtained in the domain of MPAs, as is described in Section 3. Finally, Section 4 gives a brief summary of the paper.

2. RANGE OF PRINCIPAL ANGLES FOR A GIVEN PSEUDO-BREWSTER ANGLE

All possible values of complex $\varepsilon=(\varepsilon_r,\varepsilon_i)$ for which the PBA ϕ_{pB} is one and the same are obtained as follows [14]:

$$\varepsilon_r = |\varepsilon|\cos\theta, \qquad \varepsilon_i = |\varepsilon|\sin\theta, \tag{11}$$

$$|\varepsilon| = \ell\cos(\zeta/3),$$

$$\ell = \frac{2u[1-(2u/3)]^{1/2}}{(1-u)},$$

$$\zeta = \cos^{-1}\left(-\frac{(1-u)\cos\theta}{[1-(2u/3)]^{3/2}}\right),$$

$$u = \sin^2\phi_{pB}, \qquad 0 \leqslant \theta \leqslant 180°. \tag{12}$$

As θ is increased from 0 to 180°, the minimum reflectance $|r_p|_{\min}$ at the same ϕ_{pB} increases monotonically from 0 to 1 [15]. For given ϕ_{pB}, and for each θ from 0 to 180° in steps of 1° $\varepsilon=(\varepsilon_r,\varepsilon_i)$ is calculated using Eqs. (11) and (12) and the corresponding values of $\bar{\phi}$ are determined from Eqs. (7)–(9).

In Fig. 2 the difference $\bar{\phi}-\phi_{pB}$ is plotted as a function of θ, $0\leqslant\theta\leqslant 180°$, for constant values of ϕ_{pB} from 25° to 85° in equal steps of 5°. For each ϕ_{pB} in this range, there is only one PA, $\bar{\phi}>\phi_{pB}$, and the difference $\bar{\phi}-\phi_{pB}$ increases monotonically as a function of θ. In Fig. 2 the curve for $\phi_{pB}=85°$ almost coincides with the θ axis.

From Fig. 2 it is also apparent that the maximum difference $(\bar{\phi}-\phi_{pB})_{\max}$ occurs at $\theta=180°$ and that

$$\partial(\bar{\phi}-\phi_{pB})/\partial\theta = 0, \qquad \theta = 0, 180° \tag{13}$$

At the limiting angle $\theta=180°$, Eqs. (11) and (12) yield $\varepsilon_i=0$ and $\varepsilon_r<0$ given by

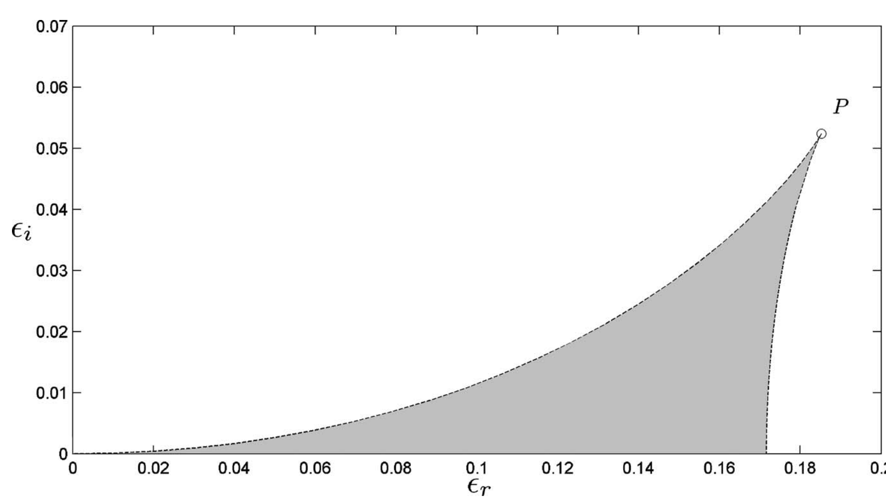

Fig. 1. Domain of MPAs, shown highlighted, is bounded by the real axis, $\varepsilon_i=0$, and the dashed curve described by Eqs. [10]. Cusp point P is located at $\varepsilon=(5/27,\sqrt{2}/27)=(0.1852,0.0524)$.

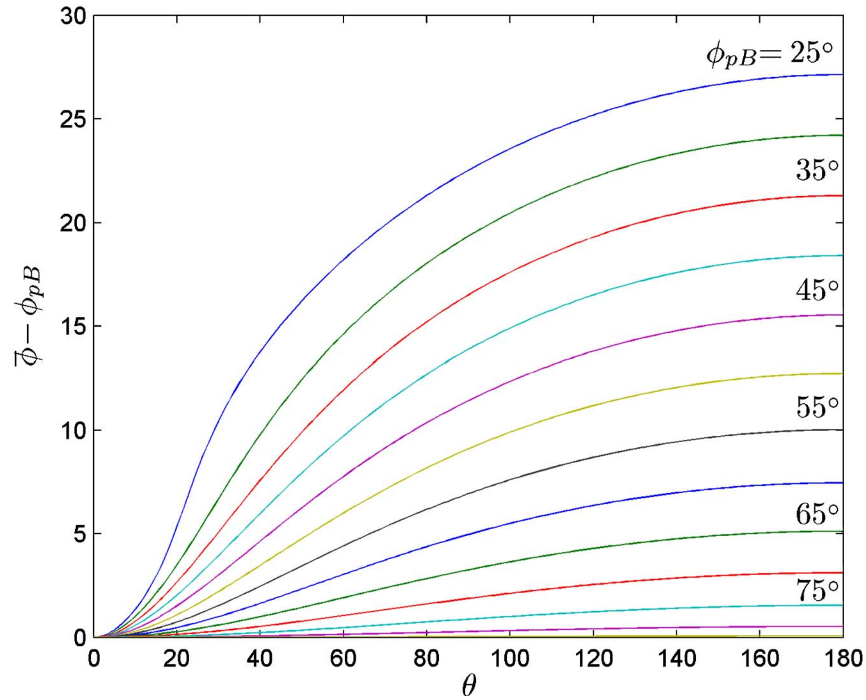

Fig. 2. (Color online) Difference of PA and PBA $\bar{\phi}-\phi_{pB}$ plotted as a function of the angle θ of complex ε, $0\leq\theta\leq180°$, for constant values of ϕ_{pB} from 25° to 85° in equal steps of 5°.

$$\varepsilon=\varepsilon_r=-\frac{1}{2}\tan^2\phi_{pB}[1+(9-8\sin^2\phi_{pB})^{1/2}]. \quad (14)$$

The maximum PA $\bar{\phi}$ that corresponds to ε_r of Eq. (14) is given by

$$\bar{\phi}_{\max}=\sin^{-1}\left\{\frac{1}{2}[(\varepsilon_r+1)+(\varepsilon_r^2-6\varepsilon_r+1)^{1/2}]^{1/2}\right\}. \quad (15)$$

The maximum difference $(\bar{\phi}-\phi_{pB})_{\max}$ calculated from Eqs. (14) and (15) is 24.207°, 15.540°, 7.458°, and 0.073° when ϕ_{pB}=30°, 45°, 60°, and 85°, respectively. Figure 3

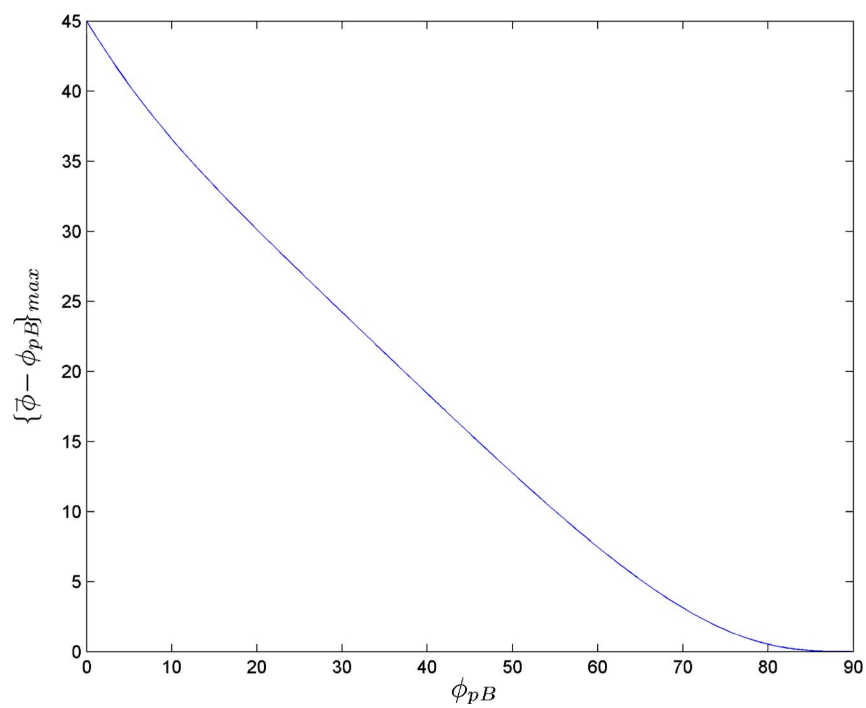

Fig. 3. (Color online) Maximum difference $(\bar{\phi}-\phi_{pB})_{\max}$ as a function of ϕ_{pB} over the entire range $0<\phi_{pB}<90°$.

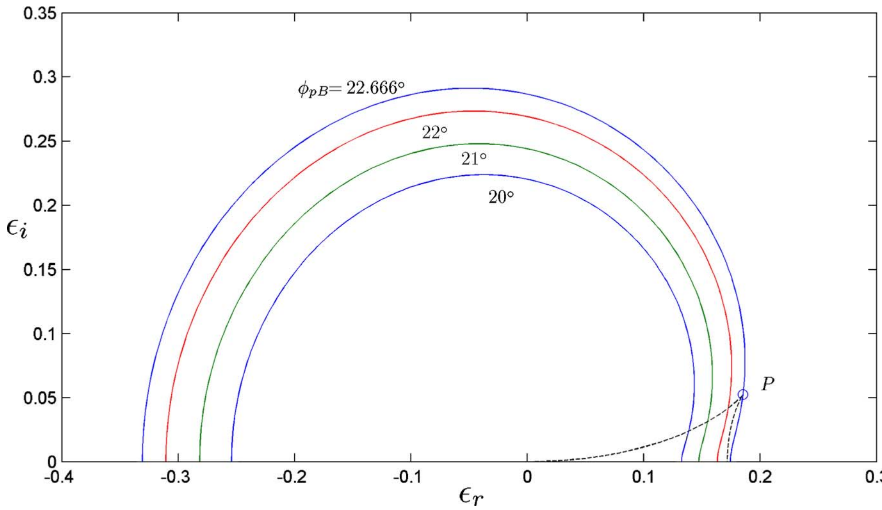

Fig. 4. (Color online) Constant-pseudo-Brewster-angle contour (CPBAC) in the complex ε plane that corresponds to $\phi_{pB}=20°$, 21°, 22°, and 22.666°. The CPBAC at $\phi_{pB}=22.666°$ passes through the cusp point P.

shows $(\bar{\phi}-\phi_{pB})_{\max}$ plotted versus ϕ_{pB} over the entire range $0<\phi_{pB}<90°$. Notice that $(\bar{\phi}-\phi_{pB})_{\max}=45°$ in the limit as $\phi_{pB}\to 0$ and that $(\bar{\phi}-\phi_{pB})_{\max}=0$ in the limit as $\phi_{pB}\to 90°$. The latter limit is approached by metals in the far IR [9].

3. DOMAIN OF MULTIPLE PRINCIPAL ANGLES

MPAs exist when the PBA falls in the range

$$0<\phi_{pB}<22.666°. \tag{16}$$

Figure 4 shows four constant-PBA contours (CPBAC) in the complex ε plane that correspond to $\phi_{pB}=20°$, 21°, 22°, and 22.666°. The CPBAC at $\phi_{pB}=22.666°$ passes through the cusp point P on the boundary curve of the domain of MPAs (Fig. 1). The squared sine of this particular angle ($\phi_{pB}=22.666°$) satisfies the following cubic equation [14]:

$$324u^3-80u^2-2u+1=0. \tag{17}$$

As an example of MPAs, consider $\varepsilon=(0.1349, 0.0118)$, which corresponds to $\theta=5°$ on the CPBAC $\phi_{pB}=20°$. For this value of complex ε, Fig. 5 shows $|r_p|$, $|r_s|$, and Δ as functions of the angle of incidence ϕ. The minimum reflec-

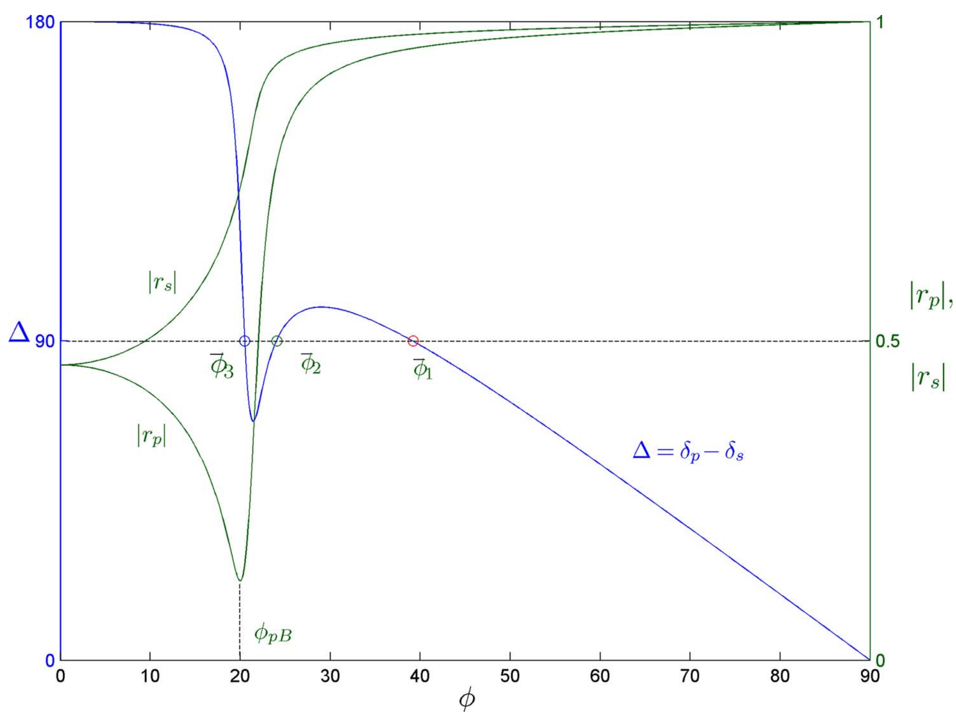

Fig. 5. (Color online) Amplitude reflectances $|r_p|$, $|r_s|$ and differential reflection phase shift Δ plotted as functions of the angle of incidence ϕ when $\varepsilon=(0.1349, 0.0118)$. Minimum reflectance $|r_p|_{\min}$ is located at $\phi=\phi_{pB}=20°$, and $\Delta=90°$ occurs at three distinct PAs: $\bar{\phi}_1=39.13°$, $\bar{\phi}_2=24.01°$, and $\bar{\phi}_3=20.49°$.

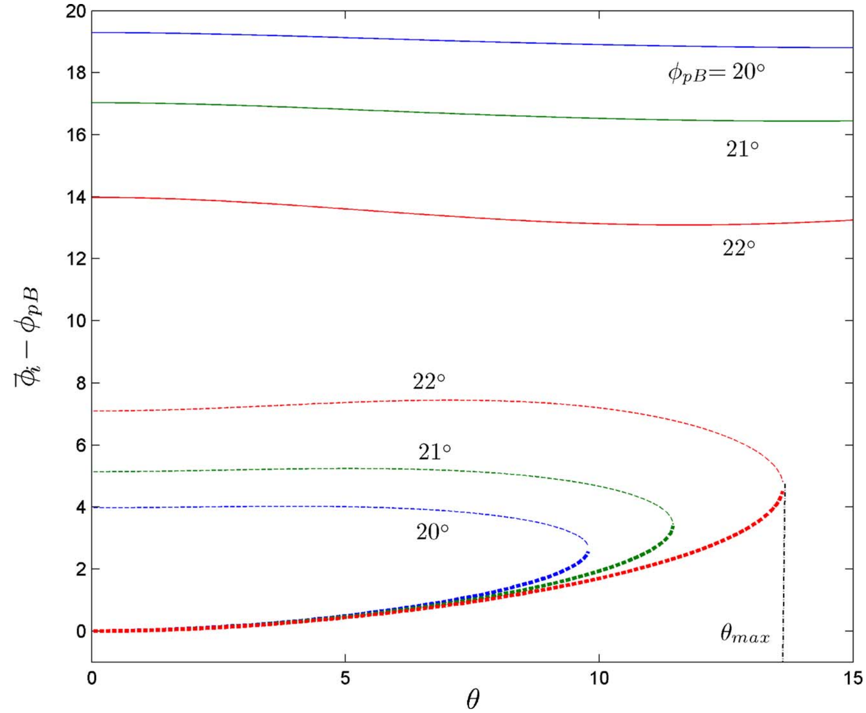

Fig. 6. (Color online) Multiple solution branches of the difference function $\bar{\phi}_i-\phi_{pB}$, $i=1,2,3$, plotted versus the angle θ of complex ε, for $\phi_{pB}=20°$, 21°, and 22°. For each ϕ_{pB} the solid, thin-dashed, and thick-dashed curves correspond to $\bar{\phi}_1>\bar{\phi}_2>\bar{\phi}_3$.

tance $|r_p|_{\min}$ appears at $\phi=\phi_{pB}=20°$, and $\Delta=90°$ occurs at three distinct PAs: $\bar{\phi}_1=39.13°$, $\bar{\phi}_2=24.01°$, and $\bar{\phi}_3=20.49°$. All three PAs $\bar{\phi}_i$, $i=1,2,3$, are $>\phi_{pB}$, which is true for any complex ε.

Figure 6 shows multiple solution branches $\bar{\phi}_i-\phi_{pB}$, $i=1,2,3$, as functions of θ for $\phi_{pB}=20°$, 21°, and 22°. For each ϕ_{pB} the solid, thin-dashed, and thick-dashed curves correspond to $i=1,2,3$, respectively, where $\bar{\phi}_1>\bar{\phi}_2>\bar{\phi}_3$. MPAs exist over a small range of θ, $0\leq\theta\leq\theta_{\max}$, where $\theta_{\max}$ is a function of ϕ_{pB}. Note that $\bar{\phi}_3-\phi_{pB}$ is almost independent of ϕ_{pB} for small θ ($<7°$). Also note that Eq. (13) is again satisfied at $\theta=0$.

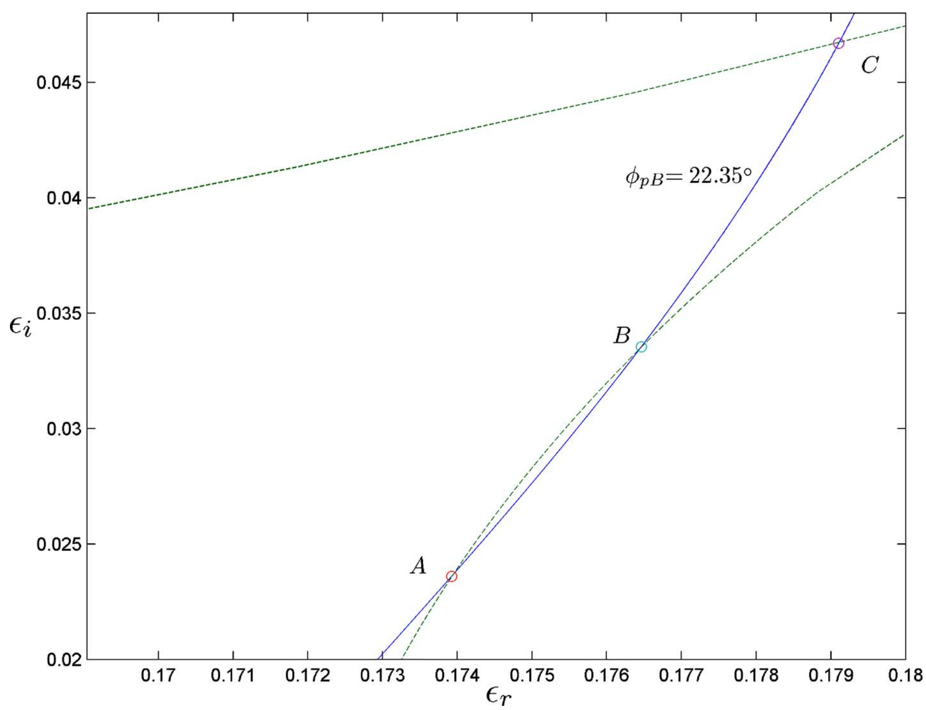

Fig. 7. (Color online) CPBAC for $\phi_{pB}=22.35°$. This curve intersects the boundary of the domain of MPAs at three points, A, B, and C, where $\theta_A=7.730°$, $\theta_B=10.763°$, $\theta_C=14.614°$.

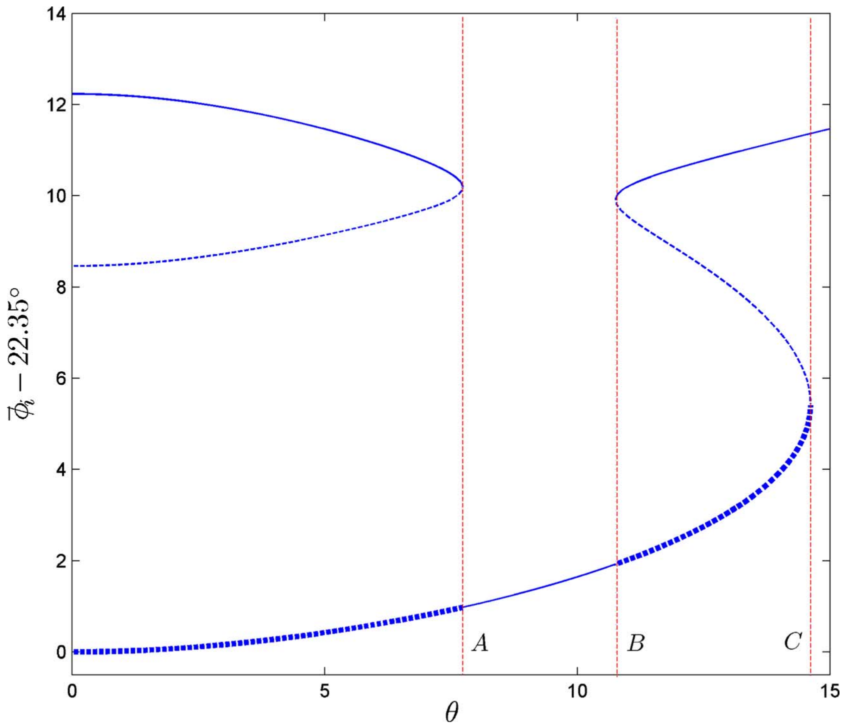

Fig. 8. (Color online) Multiple solution branches of the difference function $\bar{\phi}_i - \phi_{pB}$, $i=1,2,3$, plotted versus the angle θ of complex ε when $\phi_{pB}=22.35°$. For this PBA, MPAs exist for $0 \leqslant \theta \leqslant \theta_A$ and $\theta_B \leqslant \theta \leqslant \theta_C$, whereas one PA appears when $\theta_A < \theta < \theta_B$ and $\theta > \theta_C$.

More complex behavior is encountered in a very narrow range of the PBA, $22.339° < \phi_{pB} < 22.5°$ Figure 7 shows the CPBAC for $\phi_{pB}=22.35°$. This curve intersects the boundary of the region of MPAs at three points A, B, and C where $\theta_A=7.730°$, $\theta_B=10.763°$, $\theta_C=14.614°$.

Figure 8 shows $\bar{\phi}_i - \phi_{pB}$, $i=1,2,3$, as functions of θ when $\phi_{pB}=22.35°$. For this PBA, MPAs exist for $0 \leqslant \theta \leqslant \theta_A$ and $\theta_B \leqslant \theta \leqslant \theta_C$, whereas one PA appears when $\theta_A < \theta < \theta_B$ and $\theta > \theta_C$.

Finally, Fig. 9 shows a composite plot of multiple solution branches of the difference function $\bar{\phi}_i - \phi_{pB}$, $i=1,2,3$, versus θ for $\phi_{pB}=21°$, 22°, 22.3°, 22.35°, 22.5°, and

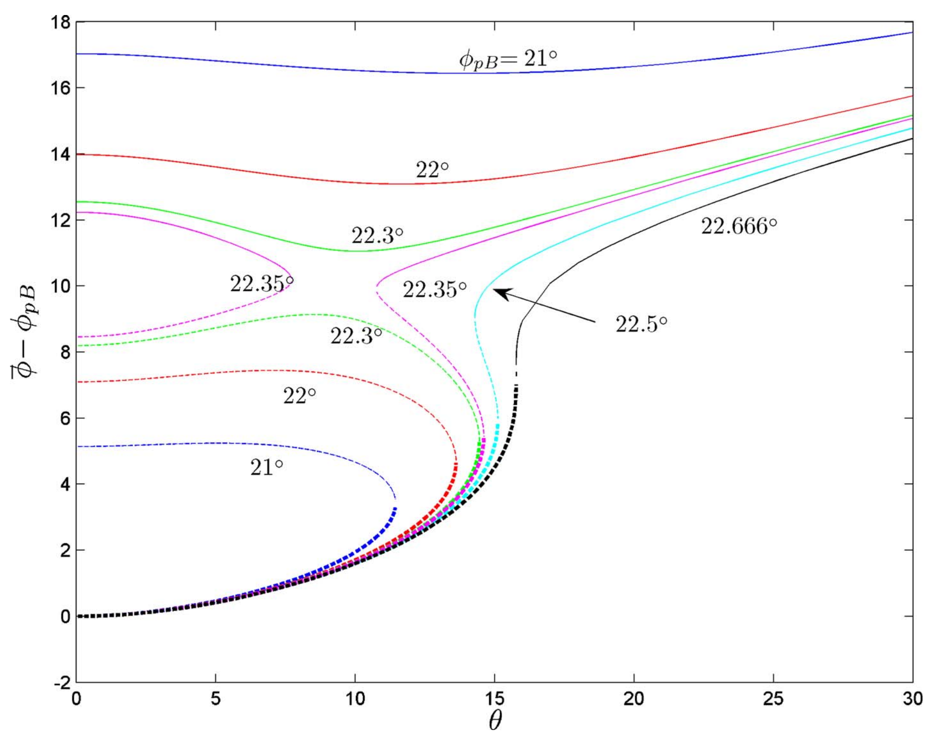

Fig. 9. (Color online) Composite plot of multiple solution branches of the difference functions $\bar{\phi}_i - \phi_{pB}$, $i=1,2,3$, for $\phi_{pB}=21°$, 22°, 22.3°, 22.35°, 22.5° and 22.666° in the domain of MPAs.

22.666° in the domain of MPA. As in Fig. 6, for each ϕ_{pB} the solid, thin-dashed, and thick-dashed curves correspond to $\bar{\phi}_1 > \bar{\phi}_2 > \bar{\phi}_3$. Again, notice that $\bar{\phi}_3 - \phi_{pB}$ is almost independent of ϕ_{pB} for small θ (<7°).

4. SUMMARY

The main conclusions of this work are summarized below:

(1) Whereas there is only one unique pseudo-Brewster angle ϕ_{pB} that characterizes a given dielectric–conductor interface, one, two, or three principal angles $\bar{\phi}_i > \phi_{pB}$, $i = 1, 2, 3$, may exist for the same complex ε.

(2) For a fixed ϕ_{pB} there is a spread of each of the three possible associated principal angles $\bar{\phi}_i$, $i = 1, 2, 3$.

(3) Only one principal angle $\bar{\phi}_1$ exists per each complex ε if $\phi_{pB} > 22.666°$.

(4) The maximum difference $(\bar{\phi} - \phi_{pB})_{\max}$ for a given ϕ_{pB} occurs when ε becomes real negative and is determined by Eqs. (14) and (15). $(\bar{\phi} - \phi_{pB})_{\max} \rightarrow 45°$ and 0 in the limit as $\phi_{pB} \rightarrow 0$ and 90°, respectively.

(5) For $\phi_{pB} \geqslant 85°$, we find that $(\bar{\phi} - \phi_{pB})_{\max} < 0.1°$.

(6) Complex behavior of the difference function $\bar{\phi}_i - \phi_{pB}$, $i = 1, 2, 3$, is encountered in the domain of fractional optical constants as is illustrated by Figs. 6 and 9.

REFERENCES

1. M. Born and E. Wolf, *Principles of Optics* (Cambridge U. Press, 1999).
2. R. M. A. Azzam and N. M. Bashara, *Ellipsometry and Polarized Light* (North-Holland, 1987).
3. J. Lekner, *Theory of Reflection* (Martinus, Nijhoff, 1987).
4. S. P. F. Humphreys-Owen, "Comparison of reflection methods for measuring optical constants without polarimetric analysis, and proposal for new methods based on the Brewster angle," Proc. Phys. Soc. London **77**, 949–957 (1961).
5. H. B. Holl, "Specular reflection and characteristics of reflected light," J. Opt. Soc. Am. **57**, 683–690 (1967).
6. G. P. Ohman, "The pseudo-Brewster angle," IEEE Trans. Antennas Propag. **AP-25**, 903–904 (1977).
7. R. M. A. Azzam, "Maximum minimum reflectance of parallel-polarized light at interfaces between transparent and absorbing media," J. Opt. Soc. Am. **73**, 959–962 (1983).
8. S. Y. Kim and K. Vedam, "Analytic solution of the pseudo-Brewster angle," J. Opt. Soc. Am. A **3**, 1772–1773 (1986).
9. L. R. Hooper, J. R. Sambles, and A. P. Bassom, "The transverse magnetic reflectivity minimum of metals," Opt. Express **16**, 7580–7586 (2008).
10. R. M. A. Azzam, "Contours of constant principal angle and constant principal azimuth in the complex ε plane," J. Opt. Soc. Am. **71**, 1523–1528 (1981).
11. E. D. Palik, ed., *Handbook of Optical Constants of Solids* (Academic, 1985).
12. D. L. Windt, W. C. Cash, Jr., M. Scott, P. Arendt, B. Newman, R. F. Fisher, A. B. Swartzlander, P. Z. Takacs, and J. M. Pinneo, "Optical constants for thin films of C, diamond, Al, Si, and CVD SiC from 24 Å to 1216 Å," Appl. Opt. **27**, 279–295 (1988).
13. R. M. A. Azzam, "Differential reflection phase shift under conditions of attenuated internal reflection," J. Opt. Soc. Am. A **16**, 1700–1702 (1999).
14. R. M. A. Azzam and E. Ugbo, "Contours of constant pseudo-Brewster angle in the complex ε plane and an analytical method for the determination of optical constants," Appl. Opt. **28**, 5222–5228 (1989).
15. R. M. A. Azzam and E. Ugbo, "Angular range for reflection of p-polarized light at the surface of an absorbing medium with reflectance below that at normal incidence," J. Opt. Soc. Am. A **19**, 112–115 (2002).